

PIN protein phosphorylation by plant AGC3 kinases and its role in polar auxin transport Huang, F.

Citation

Huang, F. (2010, September 1). PIN protein phosphorylation by plant AGC3 kinases and its role in polar auxin transport. Retrieved from https://hdl.handle.net/1887/15916

Version: Not Applicable (or Unknown)

License: <u>Leiden University Non-exclusive license</u>

Downloaded from: https://hdl.handle.net/1887/15916

Note: To cite this publication please use the final published version (if applicable).

Chapter 2

Phosphorylation of conserved PIN motifs directs *Arabidopsis* PIN1 polarity and auxin transport

Fang Huang, Marcelo Kemel Zago, Arnoud van Marion, Carlos Samuel Galván Ampudia and Remko Offringa

Modified from Huang et al., (2010) The Plant Cell 22, 1129-1142

Abstract

Polar cell-to-cell transport of auxin by plasma membrane-localized PIN-FORMED (PIN) auxin efflux carriers generates auxin gradients that provide positional information for various plant developmental processes. The apical-basal polar localization of the PIN proteins that determines the direction of auxin flow is controlled by reversible phosphorylation of the PIN hydrophilic loop (PINHL). Here, we identified three evolutionarily conserved TPRXS(N/S) motifs within the PIN1HL, and proved that the central serine residues were phosphorylated by the PINOID (PID) kinase. Loss-ofphosphorylation PIN1:GFP protein (serine to alanine) induced inflorescence defects, correlating with their basal localization in the shoot apex, and induced internalization of PIN1:GFP during embryogenesis, leading to strong embryo defects. Conversely, phosphomimic PIN1:GFP (serine to glutamic acid) showed apical localization in the shoot apex but did not rescue pin1 inflorescence defects. Both loss-of-phosphorylation and phosphomimic PIN1:GFP proteins were insensitive to PID overexpression. The basal localization of loss-of-phosphorylation PIN1:GFP increased auxin accumulation in the root tips, partially rescuing PID overexpression-induced root collapse. Collectively, our data indicate that reversible phosphorylation of the conserved serines in the PIN1HL by PID (and possibly by other AGC kinases) is required and sufficient for proper PIN1 localization, and is thus essential for generating the differential auxin distribution that directs plant development.

Introduction

The plant hormone auxin plays a central role in almost all aspects of plant development. Unidirectional cell-to-cell transport of auxin generates maxima and minima that are instrumental for tropic growth responses, tissue patterning and organ initiation (Sabatini et al., 1999; Friml et al., 2002b; Benková et al., 2003; Friml et al., 2003b; Sorefan et al., 2009). The polar auxin flow is accomplished by the concerted action of three families of membrane proteins, the AUXIN RESISTANT 1/LIKE AUX1 (AUX1/LAX) influx carriers (Parry et al., 2001b), the PIN-FORMED (PIN) efflux carriers (Paponov et al., 2005), and the P-GLYCOPROTEIN (PGP/ABCB) transporters (Geisler and Murphy, 2006). Until now the role of the PIN auxin efflux carriers in polar auxin transport is most well-established. The *Arabidopsis thaliana* genome encodes eight PIN proteins, named after the *pin-formed/pin1* mutant that is defective in polar auxin transport and develops pin-shaped inflorescences (Gälweiler et al., 1998). The PIN family proteins can be classified into two groups: i) the PIN1-type proteins (PIN1, 2, 3, 4, and 7) that are plasma membrane (PM)

localized and ii) the PIN5-type proteins (PIN5, 6 and 8) that localize to the endoplasmatic reticulum (ER) and seem to be involved in the regulation of auxin homeostasis (Mravec et al., 2009). The PIN1-type proteins have redundant functions, and a loss-of-function mutation in one *PIN* gene is sometimes compensated for by the ectopic expression of other PINs (Blilou et al., 2005; Vieten et al., 2005). As a result, only mutants in multiple *PIN* genes show more pronounced phenotypes in embryogenesis, root patterning and lateral root initiation (Benková et al., 2003; Friml et al., 2003b; Blilou et al., 2005).

The PIN1-type proteins determine the direction of cell-to-cell auxin transport through their asymmetric subcellular localization at the PM, which is dependent not only on tissue-specific factors, but also on the PIN protein sequence (Wiśniewska et al., 2006). During specific developmental processes, dynamic changes in PIN polarity have been observed (Benková et al., 2003; Friml et al., 2003b; Heisler et al., 2005), and PIN polarity has also been shown to be modulated by environmental cues (Friml et al., 2002b; Harrison and Masson, 2008) and auxin itself (Paciorek et al., 2005; Sauer et al., 2006). Many research efforts have focused on what determines PIN polarity, and thus what translates upstream developmental and environmental signals into changes in plant architecture by regulating PIN polarity. The current model is that newly synthesized PINs arrive at the PM in a non-polar fashion, and that PIN polarity is established and regulated by subsequent endocytosis, transcytosis and recycling back to the PM (Geldner et al., 2001; Dhonukshe et al., 2008; Kleine-Vehn et al., 2008a).

GNOM is a GDP/GTP exchange factor on ADP-ribosylation factor G protein (ARF-GEF) that has been shown to be involved in the recycling of PIN proteins to the basal (root apex facing) side of the PM (Geldner et al., 2003). GNOM is a molecular target of the fungal toxin brefeldin A (BFA), which inhibits protein trafficking and thus interferes with basal PIN1 recycling, leading to PIN1 accumulation into so-called BFA compartments (Geldner et al., 2001). Loss-of-function of *GNOM* results in severe embryo defects due to disturbance of PIN1 polarity establishment during embryogenesis (Mayer et al., 1993; Steinmann et al., 1999).

Another important molecular determinant in PIN polar targeting is the PINOID (PID) protein serine/threonine kinase. PID was initially identified through the *Arabidopsis pinoid* loss-of-function mutants that phenocopy *pin1* mutants (Bennett et al., 1995; Christensen et al., 2000). Both *PID* loss- and gain-of-function mutants phenotypes already indicated a role of PID as a regulator of auxin transport (Benjamins et al., 2001). More recently, PID was shown to act as a binary switch in the apical-basal polar targeting of PIN proteins (Friml et al., 2004). In root cells, *PID* overexpression induces a PIN polarity shift from the basal to the apical (shoot apex facing) side of the cells, leading to agravitropic root growth and collapse of the primary root meristem, due to depletion of the organizing auxin maximum. In contrast, in the inflorescence meristem, *pid* loss-of-function induces an

apical-to-basal shift in PIN1 polarity, which drains the auxin maxima that are necessary for organ initiation, thus resulting in pin-like inflorescences (Friml et al., 2004).

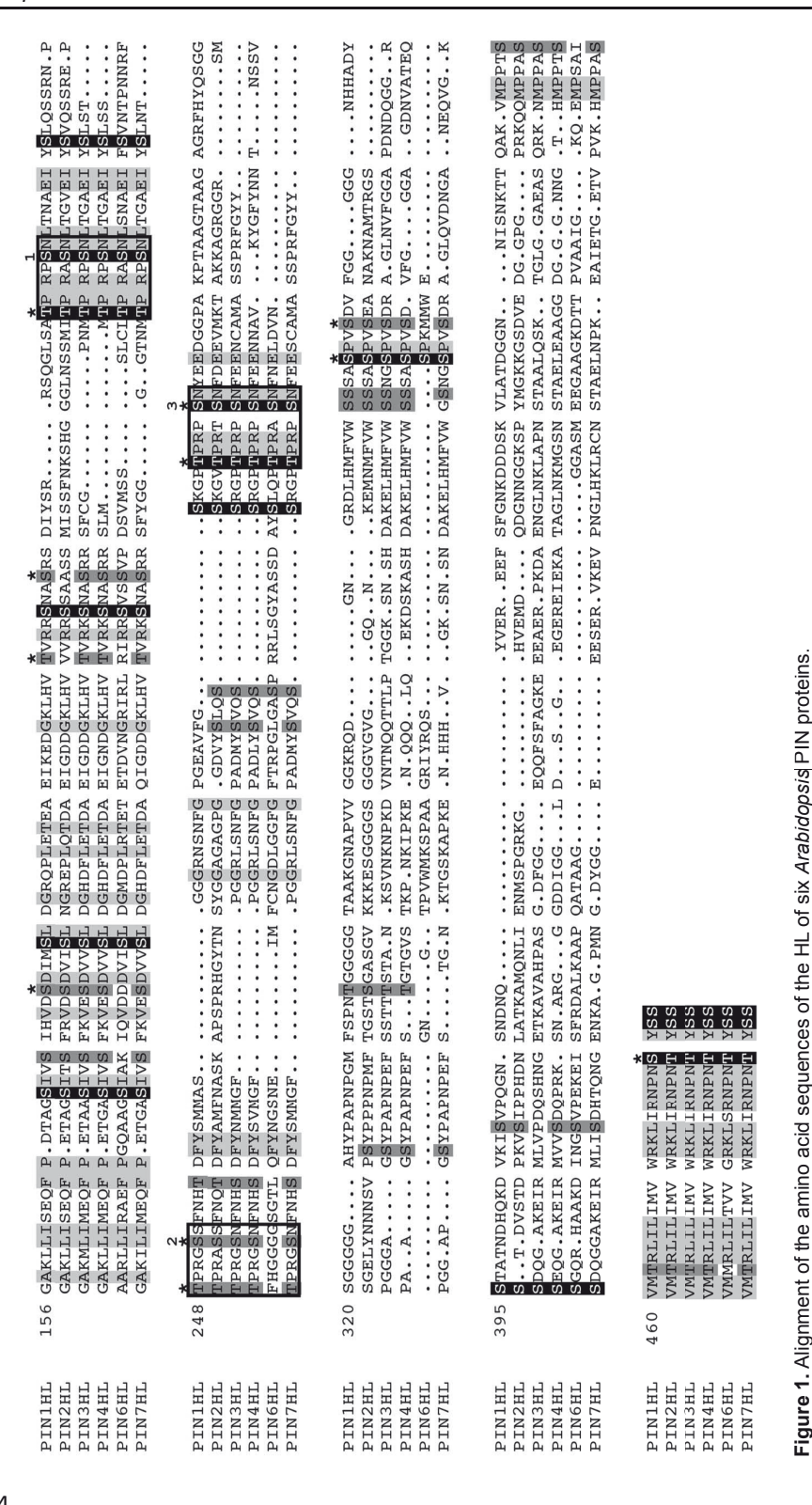
In animal systems, modification of cargo proteins by phosphorylation is an important mechanism to regulate their polar delivery to the PM. For example, in mammalian epithelial cells, phosphorylation of the immunoglobulin receptor at a single serine residue has been shown to result in its accumulation at the apical cell membrane (Casanova et al., 1990). Protein phosphorylation and dephosphorylation have also been implicated in the regulation of polar auxin transport in plant systems. In tobacco (*Nicotiana tabacum* L.) suspension cells, the protein kinase inhibitors staurosporine and K252a were found to inhibit auxin efflux (Delbarre et al., 1998), and genetic and pharmacological inhibition of phosphatase activity in *Arabidopsis* led to defects in auxin transport (Garbers et al., 1996; Rashotte et al., 2001). More recent findings revealed that PIN polar localization is determined by reversible phosphorylation of the large central PIN hydrophilic loop (PINHL) through the antagonistic action of the PID kinase and PP2A phosphatases (Michniewicz et al., 2007). This indicated that the machinery of phosphorylation–regulated PM protein polar localization is also operational in plants.

To further elucidate molecular mechanisms of PIN polar localization regulated by PID phosphorylation, we set out to identify the PID phosphorylation targets in the PINHL. Here, we show that the central serine residues in three conserved TPRXS(N/S) motifs within the PIN1HL are phosphorylated by PID. Inactivation of these phosphosites (non-phosphorylatable or phosphomimic forms) in a complementing *PIN1:GFP* construct induced auxin-regulated defects in embryo and inflorescence development that correlated with changes in PIN1:GFP polar localization. Moreover, the localization of loss-of-phosphorylation and phosphomimic PIN1:GFP proteins in root tips was insensitive to PID overexpression using *355::PID*, leading to opposite effects on *355::PID*—induced root collapse. Our data indicate that the regulation of PIN1 polar localization through reversible phosphorylation of three conserved serines in the PIN1HL by PID and possibly other AGC kinases is an essential mechanism for aspects of plant development that are directed by differential auxin distribution.

Results

Serine residues in three conserved motifs in the PIN1HL are phosphorylated by PID

The previous observations that the PIN1HL is efficiently phosphorylated by PID *in vitro* (Michniewicz et al., 2007), prompted us to map PID phosphorylation targets in the PIN1HL. Analysis of the PIN1 amino acid sequence using the NetPhos program (Blom



Conserved serines or threonines predicted by NetPhos to be phosphorylated are indicated by asterisks. Residues that are conserved in all six PINHLs are blocked with black (serines and threonines) or light gray (other amino acids). Residues that are conserved in four or five of the six PINHLs are blocked with dark gray. The three TPRXS(N/S) motifs are boxed, and the serine residues at positions 231, 252 and 290 within these motifs are renumbered to 1, 2 and 3, respectively.

et al., 1999) identified twenty-three putative phosphosites, twenty of which are located in the PIN1HL (Zago, 2006). Twelve synthetic peptides comprising seventeen putative phosphosites were tested in *in vitro* phosphorylation assays, and six were found to be highly phosphorylated by PID (Zago, 2006).

Since the PID-dependent basal-to-apical switch in PIN polarity is not restricted to PIN1. but is also observed for PIN2 and PIN4 (Friml et al., 2004), we aligned the amino acid sequences of six PIN proteins (PIN1, 2, 3, 4, 6 and 7) in which a clear HL can be identified. Eleven of the NetPhos predicted serine (S) and thrione (T) residues showed conservation among the six Arabidopsis PIN proteins (indicated with asterisk in Figure 1), five of which appeared to be fully conserved (labeled in black and asterisk in Figure 1). Interestingly, these five residues were located in the highly phosphorylated peptides 2, 6, 8, 12 (Zago, 2006), and two of them (T227 and S290) were recently reported to be modified by phosphorylation in vivo (Benschop et al., 2007). We noted that S290 was located in a TPRXSN motif that was conserved among the six PIN proteins (Figure 1) and resembled the consensus phosphorylation site of the animal AGC kinase PKA. Therefore, we first tested whether S290 is a PID phosphorylation target by replacing this serine with alanine in a HIS-tagged short version of the PIN1HL (PIN1HLsv) (Zago, 2006), and incubating wild type or mutant proteins with HIS-tagged PID in an in vitro phosphorylation reaction. Clear PID autophosphorylation and PID-dependent phosphorylation of HIS-PIN1HLsv was detected (Zago, 2006). The S290A substitution reduced PIN1 phosphorylation by PID to a background level (data not shown), indicating that S290 is a PID phosphorylation target. Two additional TPRXS(N/S) motifs were identified upstream of S290 (Figure 1), and S252 in the second motif was also shown to be modified by phosphorylation in vivo (Benschop et al., 2007). For convenience in our experiments, we refer to the serines at positions 231, 252 and 290 as S1, S2 and S3, respectively (Figure 1).

We next tested the effect of serine to alanine substitution (S1A, S2A, S3A or combinations) on PID phosphorylation using a GST-tagged version of the full length PIN1HL (Figure 2A). Under our experimental conditions, the GST-PIN1HL was unstable, showing a reproducible pattern of degradation bands. A single S1A or S3A substitution led to a 40% or 20% reduction, respectively, double S1,2A and S1,3A substitutions led to a 50% reduction, and triple S1,2,3A substitutions led to a 80% reduction of phosphorylation by PID compared to the wild type PIN1HL (Figure 2B). These data indicated that the central serine residues within the three highly conserved TPRXS(N/S) motifs are targets for PID phosphorylation *in vitro*.

At the same time, the PIN1HL S1,3A double substitution construct was used to test all other serine and threonine residues located in the highly phosphorylated peptides 2 (T227), 6 (T286), 8 (S377 and S380), 11 (T458 and S459) and 12 (S479) (Zago, 2006).

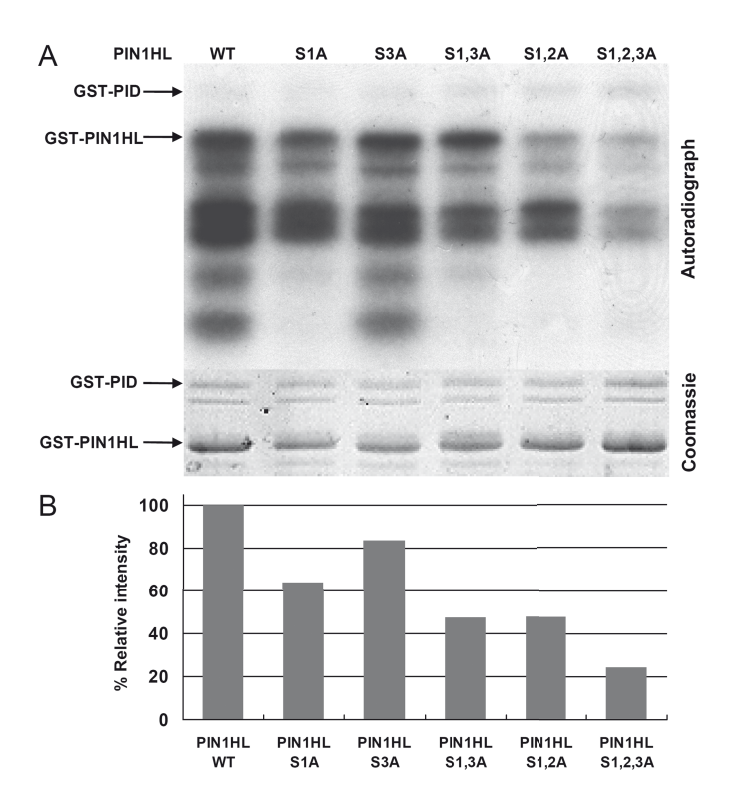


Figure 2. Serine residues in three conserved motifs within the PIN1HL are phosphorylated by PID *in vitro*. **(A)** *In vitro* assay of phosphorylation by GST-PID kinase using wild type GST-PIN1HL and mutant protein substrates in which the indicated serines (S1, S2, or S3) were replaced with alanines (A). The positions of GST-PID and the full length GST-PIN1HL are indicated in the autoradiograph (upper panel) and the Coomassie stained gel (lower panel). Autophosphorylation of GST-PID can be observed in the upper panel. Under our experimental conditions, *E. coli* purified GST-PIN1HL was not stable, resulting in a reproducible pattern of degradation bands. The coomassie stained gel was used as a control for protein loading.

(B) Quantitative assessment of the *in vitro* phosphorylation assay in **(A)**. The phosphorylation intensity is expressed as the percentage of phosphorylation relative to the wild type GST-PIN1HL protein. Numbers were corrected for protein loading based on analysis of the Coomassie stained blot.

Based on the relative intensities of the phosphorylated bands, substitution of these amino acids with alanines had no clear effect on PID phosphorylation (data not shown), indicating that these residues are not phosphorylated by PID.

BLAST analysis of the *Arabidopsis* protein database (http://www.ncbi.nlm.nih. gov/protein/) showed that TPRXS(N/S) is a PIN-specific motif. Strikingly, alignment of amino acid sequences of PIN1 proteins from five different plant species (Xu et al., 2005; Carraro et al., 2006) showed that the three identified motifs are highly conserved, even in the moss *Physcomitrella patens* (Figure 3), suggesting their functional conservation throughout the evolution of land plants.

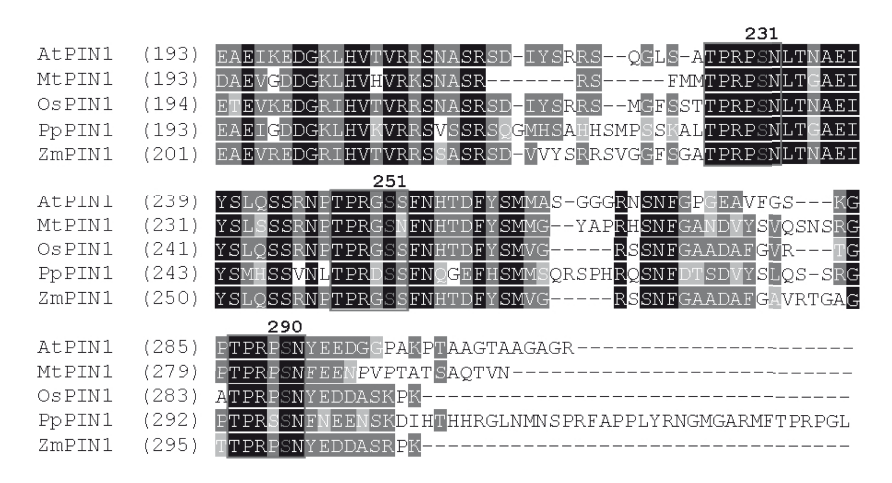


Figure 3. Alignment of the amino acid sequences of the PIN1 proteins from five plant species showing the evolutionary conservation of the three TPRXS(N/S) motifs.

Loss of PIN1 phosphorylation at the conserved serines induces dominant embryo and flower phenotypes

To investigate the biological significance of the PIN1 phosphorylation in *Arabidopsis*, various mutant constructs were generated from *PIN1::PIN1:GFP* (hereafter referred to as *PIN1:GFP*), in which one, two, or all three serine residues (S) in the encoded PIN1:GFP proteins were replaced by alanine (A), a nonphosphorylatable residue, or by glutamic acid (E) to mimick phosphorylation. The resulting constructs *PIN1:GFP S1A(E)*, *PIN1:GFP S1,3A(E)* and *PIN1:GFP S1,2,3A(E)* were transformed into *Arabidopsis* Columbia wild type (Col WT) plants, and GFP positive, single locus insertion lines were selected for analysis. A previously described *PIN1:GFP* line (Benková et al., 2003) was used as the control.

The PIN1:GFP S→E and PIN1:GFP S3A lines showed largely normal development at seedling and flowering stages. In contrast, other mutants exhibited a range of dominant defects. The PIN1:GFP S1A and PIN1:GFP S1,3A mutants showed cotyledon number defects, reflected by seedlings having one, three, or four cotyledons (Figures 4D-4F), with the three-cotyledon phenotype characteristic of the pid loss-of-function mutant (Figure 4B) predominating. For these two mutant constructs, two lines each were selected for detailed analyses, one with a lower PIN1:GFP expression level (PIN1:GFP S1A#14 and PIN1:GFP S1,3A#12) and one with a higher PIN1:GFP expression level (PIN1:GFP S1A#15 and PIN1:GFP S1,3A#10). Notably, the stronger lines showed higher frequencies of cotyledon defects (e.g. PIN1:GFP S1A#15: 21.7% n=757) than the weaker lines (e.g. PIN1:GFP S1A#14: 12.5% n=654) (Figure 4N), indicating that the severity of the cotyledon phenotypes corresponded to the level of mutant PIN1:GFP

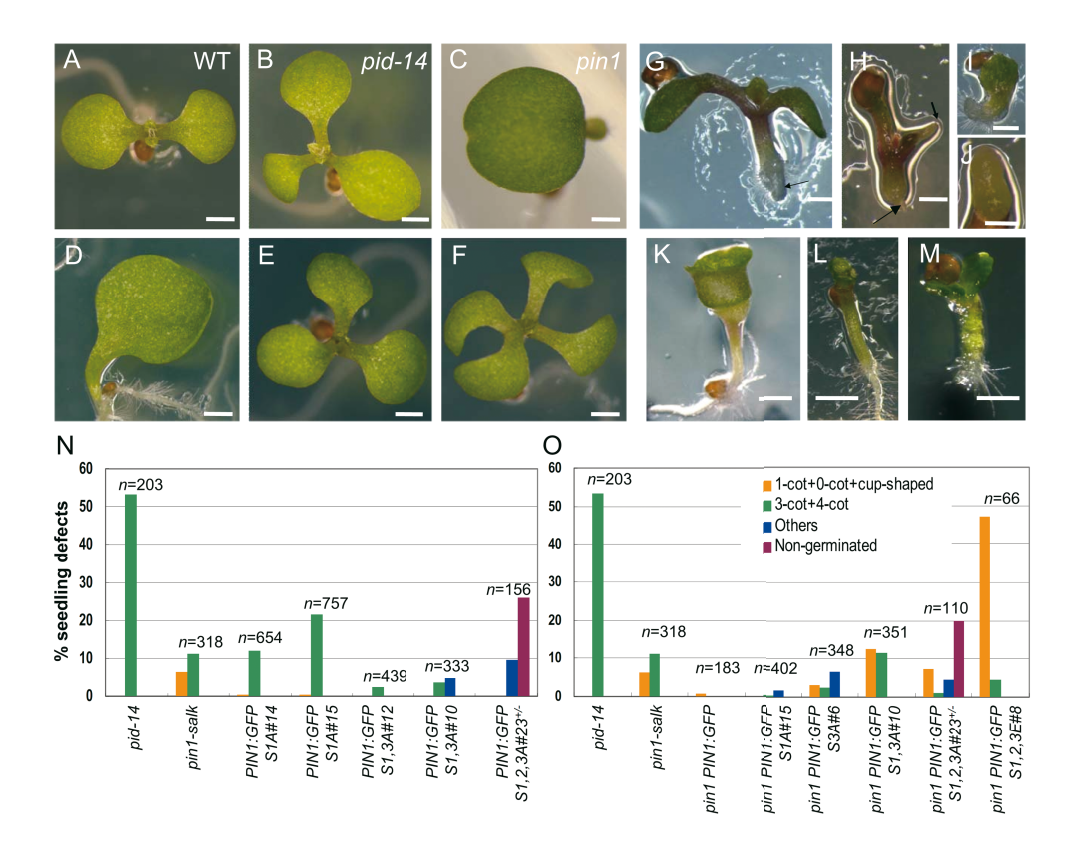


Figure 4. Seedling phenotypes induced by manipulation of the conserved serines in PIN1:GFP.

- (A) to (F) Cotyledon number defects observed in pid-14 (B), pin1 (C) and $PIN1:GFP S \rightarrow A$ ([D] to [F]) mutant seedlings compared with a WT seedling (A).
- (G) to (J) Progeny from *PIN1:GFP S1,2,3A#23**/ plants showing severe patterning defects such as seedling without a root ([G] and [H]), or with reduced cotyledons (H), or oblong structures ([I] and [J]).
- **(K)** to **(L)** Cotyledon defects observed in *pin1 PIN1:GFP S1,3A#10* mutant seedlings showing a cup-shaped cotyledon **(K)** or no cotyledons **(L)**.
- **(M)** Progeny from *pin1*** *PIN1:GFP S1,2,3A#23*** plants showing callus-like hypocotyl and cotyledons lacking a primary root.

Bars in (A) to (M) indicate 10 μ m.

(N) and **(O)** Quantitative analysis of seedling defects induced by expression of the phosphomutant PIN1:GFP versions in wild type background **(N)** and in *pin1* mutant background **(O)**. The number of seedlings scored per mutant line is indicated. The legends in **(O)** are also used for **(N)**. "Others" represents phenotypes other than cotyledon number defects, such as seedling without root, oblong structures or callus-like seedlings.

protein expression. The stronger lines *PIN1:GFP S1A#15* and *PIN1:GFP S1,3A#10* developed flowers with an increased number of petals, and a decreased number of stamens and carpels (Figure 5B; Table 1), mimicking *pid* mutant floral defects (Figure 5A; Table 1) (Bennett et al., 1995).

Table 1. Quantitative analysis of	f dominant pid-like floral organ	defects induced by $PIN1:GFP S \rightarrow A$
-----------------------------------	----------------------------------	---

_		. Total number			
Genotype	Sepal	Petal	Stamen	Carpel	of flowers
Col WT	4.00	4.00	5.80 ± 0.40	2.00	50
pid-14	2.80 ± 1.20	8.35 ± 1.42	1.10 ± 1.07	0.00	20
PIN1:GFPS1A#15	4.11 ± 0.68	5.53 ± 0.63	4.91 ± 0.85	1.52 ± 0.57	45
PIN1:GFP1,3A#10	4.08 ± 0.68	5.71 ± 1.09	4.15 ± 0.87	1.83 ± 0.33	52

Numbers are means derived from analyses of flowers from at least five plants for each genotype. Standard deviations are indicated. In the case of organ fusion in the same whorl, a fused floral organ is counted as one in that whorl. In the case of organ fusion between different whorls, fused organs are counted as one organ in the each whorl.

To exclude other possible reasons for the observed dominant phenotypes, such as co-suppression, the protein levels of the transgene and the endogenous *PIN1* gene were quantified by protein gel blot analysis. All trangenic lines showed endogenous PIN1 expression similar to that of wild type, and the mutant PIN1:GFP expression levels of the strong lines were comparable to that of the *PIN1:GFP* control line (data not shown), suggesting that the dominant developmental defects observed can be attributed to the expression of the mutant PIN1:GFP proteins that outcompete endogenous PIN1, possibly by differential localization at the PM.

For the *PIN1:GFP S1,2,3A* triple substitution lines, the post-embryo defects were more severe. No homozygous progeny could be obtained and approximately one fourth of the seeds from heterozygous plants (25.6% n=156 for line #23) failed to germinate, indicating that the homozygous progeny are embryo lethal. Among the germinating seedlings, we occasionally (9.6% n=156 for line #23) observed strong patterning defects (indicated as "others" in Figures 4N and 4O), such as seedlings without a root (Figures 4G and 4H), or ball-shaped structures without any discernible apical–basal axis that stopped growing after germination (Figures 4I and 4J).

Reversible phosphorylation of the conserved serines is necessary and sufficient for proper PIN1 localization and plant development

To further test the functionality of the loss- or gain-of-phosphorylation PIN1:GFP proteins, the PIN1:GFP and PIN1:GFP $S \rightarrow A(E)$ mutant lines were crossed with the pin1 loss-of-function mutant, and where possible, double homozygous plants were selected for analysis. The pin1 mutant has aberrant cotyledon numbers (Figures 4C, 4N and 4O) and pin-formed inflorescences with no flowers or only a few defective flowers (Okada

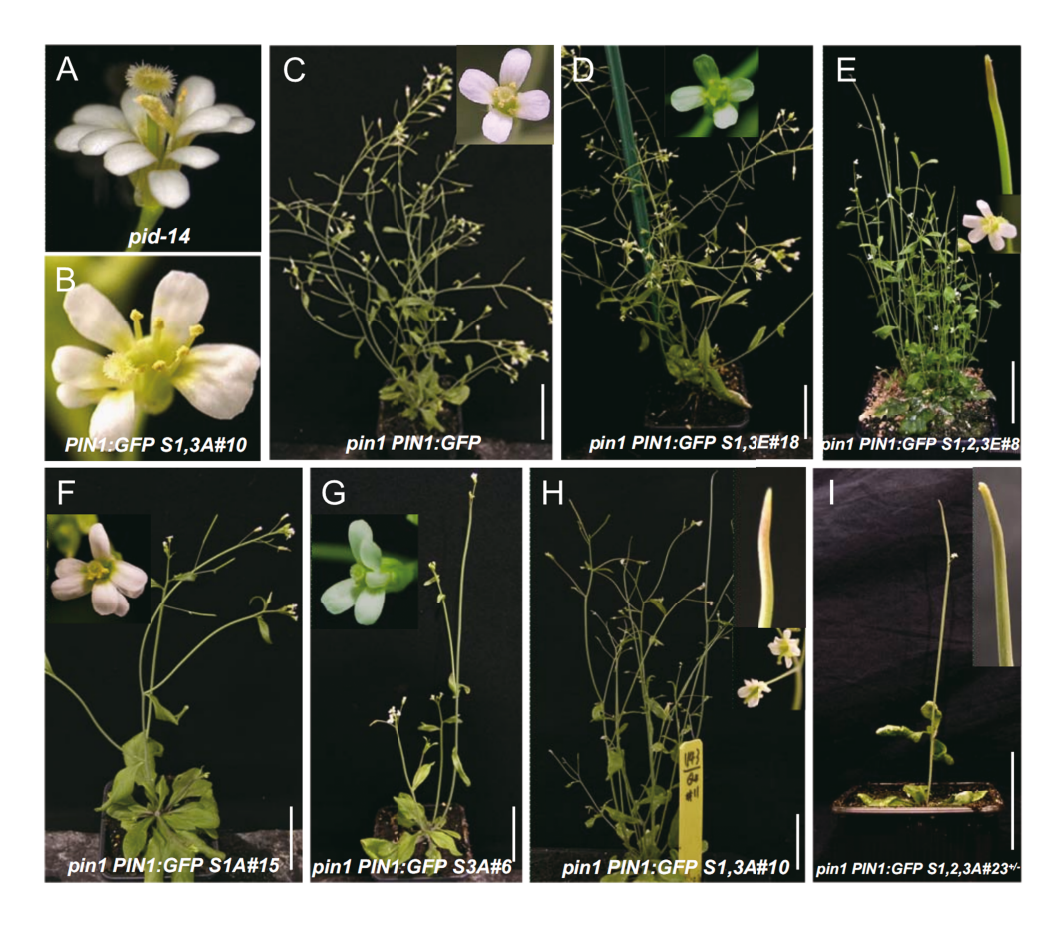


Figure 5. Inflorescence and flower defects observed after expression of phosphomutant PIN1:GFP proteins. **(A)** and **(B)** Flowers of the *pid-14* loss-of-function mutant **(A)** and the *PIN1:GFP S1,3A#10* mutant **(B)** show similar defects.

(C) to (I) Complementation analysis of *pin1* loss-of-function mutant inflorescence and flower defects. *PIN1:GFP* (C) and *PIN1:GFP S1,3E#18* (D) fully rescued pin-shaped inflorescence defects, whereas *PIN1:GFP S1A#15* (F) and *PIN1:GFP S3A#6* (G) only partially rescued pin-shaped inflorescence defects. *PIN1:GFP S1,2,3E#8* (E), *PIN1:GFP S1,3A#10* (H) and *PIN1:GFP S1,2,3A#23* (I) did not rescue *pin1*-inflorescence defects. Insets show details of flower morphology and pin-like inflorescences. Bars in whole plant photographs, 5 cm.

et al., 1991). In our analysis, *PIN1:GFP*, as well as *PIN1:GFP S1E*, *PIN1:GFP S3E* and *PIN1:GFP S1,3E*, complemented *pin1* cotyledon and inflorescence defects (Figures 4O, 5C and 5D). *PIN1:GFP S1A* and *PIN1:GFP S3A* partially rescued *pin1* defects, reflected by a reduced frequency of *pin1* cotyledon defects from 17.6% (n=318) to 2% (n=402) and 12.1% (n=348), respectively (Figure 4O), and by the observations that no pin-formed inflorescences were produced (Figures 5F and 5G). In contrast, *PIN1:GFP S1,3A* and *PIN1:GFP S1,2,3A(E)* lines showed an enhanced frequency (23.9% n=351, 32.7% n=110 and 71.2% n=66, respectively; Figure 4O) and severity of seedling defects, such as cup-

shaped cotyledons (3.5%; Figure 4K) or no cotyledons (2%; Figure 4L), phenotypes typical for the *pin1 pid* double mutant (Furutani et al., 2004), but not for the *pid* or *pin1* single mutant (Figures 4N and 4O). Around 5% of the progeny from *pin1***/ *PIN1:GFP S1,2,3A***/ (double heterozygous) plants lacked a primary root and developed callus-like hypocotyls and cotyledons (Figure 4M). At the flowering stage, *PIN1:GFP S1,3A* and *PIN1:GFP S1,2,3A(E)* mutants could not complement *pin1* defects and produced pin-like inflorescences, with *pin1 PIN1:GFP S1,2,3E* occasionally forming flowers producing seeds (Figure 5E). The *pin1 PIN1:GFP S1,3A* inflorescences were branched and formed sterile flowers with fused petals (Figure 5H), whereas *pin1 PIN1:GFP S1,2,3A**/- plants only produced a single needle-shaped inflorescence (Figure 5I).

Next, we examined whether these mutant defects correlated with changes in the subcellular localization of the mutant PIN1:GFP proteins. Consistent with previous observations (Friml et al., 2004), in auxin transport inhibitor-induced pin-shaped inflorescence apices, PIN1:GFP was localized apically in the epidermis (Figure 6A). In a comparable region of the pin-shaped inflorescence apex, the phosphomimic PIN1:GFP

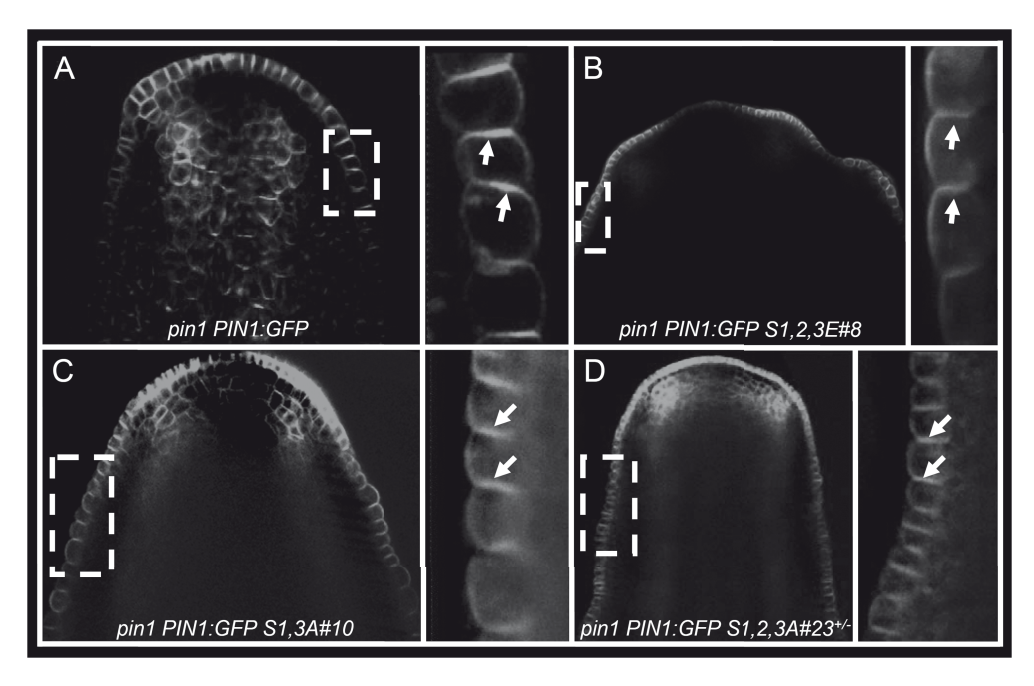


Figure 6. Subcellular localization of wild type and phosphomutant PIN1:GFP proteins in epidermal cells of the inflorescence apex.

(A) to **(D)** Confocal laser scanning microscopy of pin-formed inflorescence apices of *pin1* mutant plants expressing wild type PIN1:GFP (naphthylphthalamic acid-treated) **(A)**, PIN1:GFP S1,2,3E **(B)**, PIN1:GFP S1,3A **(C)** and PIN1:GFP S1,2,3A **(D)**. The white dashed boxes in the overview images (left) indicate the position of the zoom-in images (right). The polarity of PIN1:GFP in the epidermal cells of the inflorescence apex is indicated with arrows. *PIN1:GFP S1,2,3A#23*^{+/-} indicates that the plant is heterozygous for the transgene.

S1,2,3E protein also showed apical localization (Figure 6B), whereas the PIN1:GFP S1,3A and PIN1:GFP S1,2,3A proteins were targeted to the basal side (Figures 6C and 6D), similar to PIN1 localization in *pid* mutant (Friml et al., 2004).

Collectively, these data indicated that PIN1 loss of phosphorylation results in its basal localization, whereas phosphomimicking induces apical targeting of PIN1 in the shoot apical meristem, both leading to failure to complement the *pin1* mutant phenotypes. These observations are consistent with the identified role for PID as a binary switch in PIN1 basal-apical polar localization in the shoot apex, suggesting that the identified Ser residues are PID-related.

Strong embryo defects are induced by PIN1:GFP S1,2,3A mislocalization

The embryo and seedling lethality observed in the progeny of *pin1**/- *PIN1:GFP S1,2,3A**/- plants led us to study the early embryo development. Compared with *pin1 PIN1:GFP* embryos that showed stereotypic patterns of cell divisions (Figure 7A), about 30% (n=86) of the embryos from *pin1**/- *PIN1:GFP S1,2,3A**/- plants exhibited a range of developmental aberrations at different stages (Figure 7B). In 15% of the embryos, the basal tier and suspensor cells showed defective cell divisions. The most severe cases were characterized by embryos with globular structures that lacked a defined apical-basal axis and bilateral symmetry (5%). These embryo phenotypes resembled those of mutants with defects in auxin transport (Friml et al., 2003b) and *gnom* mutants (Mayer et al., 1993).

Examination of the subcellular localization of PIN1:GFP S1,2,3A during embryogenesis showed that PIN1:GFP S1,2,3A polarity failed to establish properly (n=43). Endogenous PIN1 (or wild type PIN1:GFP) proteins localize at the basal side of the provascular cells (Figure 7C), generating an auxin maximum that defines the hypophyseal cell group (Figure 7F), and at the apical side of the epidermal cells from triangular stage on (Figure 7C and inset), generating strong auxin activity at tips of developing cotyledons (Steinmann et al., 1999; Friml et al., 2003b). In embryos from pin1** PIN1:GFP S1,2,3A** plants with a largely wild type morphology (65% n=43), the basal PIN1:GFP localization in the provascular cells was lost (Figure 7D, star), causing a reduction of the auxin reporter DR5::GFP signal in the hypophysis (Figure 7G). As a comparison, the basal localization of PIN1:GFP S1,3A in the provascular cells was not changed (data not shown). In embryos exhibiting strong defects, PIN1:GFP S1,2,3A polarity was dramatically disrupted and abundant intracellular signal was observed (Figures 7E). The cells with the fluorescent signal at the PM showed no polarity or randomized polarity (Figures 7E), and a clear DR5::GFP maximum was not detected (Figure 7H).

These data implied that phosphorylation of the three serines is required for auxin-

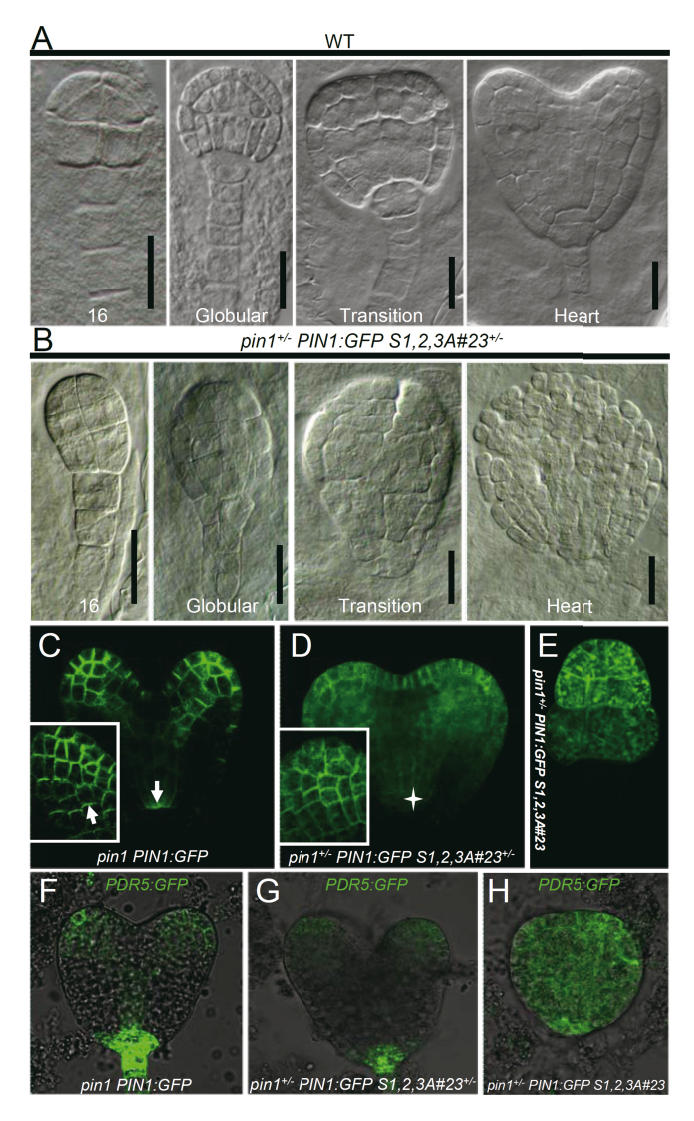


Figure 7. Embryo defects induced by PIN1:GFP S1,2,3A mislocalization are due to disturbed auxin distribution. **(A)** and **(B)** Differential interference contrast microscopy images of embryos from wild type **(A)** and $pin1^{+/-}$ $PIN1:GFP S1,2,3A\#23^{+/-}$ **(B)** plants. Text at the bottom of each image indicates the developmental stage of the embryo. For the defective embryos in **(B)** the developmental stage was based on a rough estimate of the cell number. Bars in **(A)** and **(B)**, 10 µm.

(C) to **(E)** Confocal laser scanning microscopy images of *pin1 PIN1:GFP* heart stage embryos **(C)**, and wild type looking **(D)** and defective looking **(E)** embryos from *pin1** *PIN1:GFP S1,2,3A#23** plants from the same developmental stage. Insets in **(C)** and **(D)** represent confocal scans through the epidermal cell layer of cotyledon primordia. White arrows in **(C)** and **(D)** indicate the PIN1:GFP polarity, and a star in **(D)** indicates the absence of basally localized PIN1:GFP S1,2,3A protein.

(**F**) to (**H**) Confocal laser scanning microscopy images of *PDR5:GFP* auxin distribution in embryos from *pin1 PIN1:GFP* (**F**) and *pin1*** *PIN1:GFP S1,2,3A#23*** ([**G**] and [**H**]) plants, showing a reduced (**G**) or mislocalized (**H**) auxin maximum.

related embryo development by regulating PIN1 PM localization.

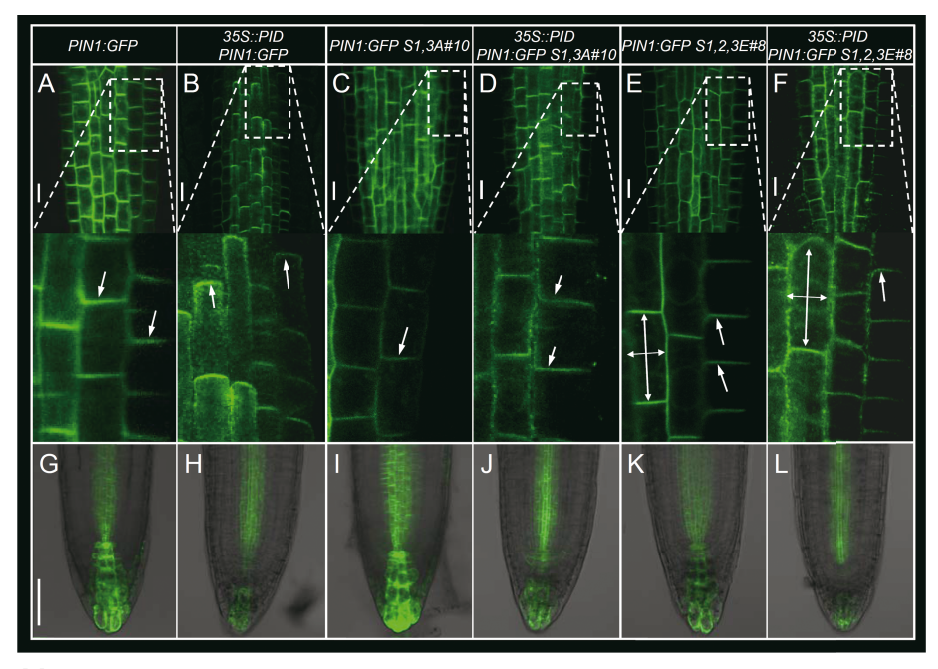
PIN1 phosphorylation at the conserved serines is related to PID activity

Above, we showed that the conserved serines are phosphorylated by PID *in vitro*, and that PID regulation of PIN1 polarity and the resulting inflorescence development (Friml et al., 2004) can be mimicked by manipulation of these Ser residues. For additional confirmation that our identified phosphoserines are targets of PID activity *in vivo*, we crossed the *PIN1:GFP*, *PIN1:GFP S1,3A* and *PIN1:GFP S1,2,3E* lines with the strong *PID* overexpression line 35S::PID#21 (Benjamins et al., 2001). The *PIN1:GFP S1,2,3A* line could not be used for this purpose, as it could only be maintained in the heterozygous state, which precluded an equivalent comparison of the root meristem collapse frequency.

In line with our previous observations (Friml et al., 2004), PID overexpression induced a clear basal-to-apical shift of PIN1:GFP localization in root stele cells (Figures 8A and 8B). In contrast, PIN1:GFP S1,3A showed basal localization in both wild type and 35S::PID backgrounds (Figures 8C and 8D). Simultaneous immunolocalization showed the basal-to-apical polarity shift of PIN2 in the cortex and PIN4 in the root meristem (Figures 9A and 9B), demonstrating that PID overexpression was sufficient to induce PIN polarity shifts, and that the S1,3A substitutions rendered PIN1:GFP insensitive to that. On the other hand, the PIN1:GFP S1,2,3E protein exhibited apical localization in some cell files, and apolar localization in others in both wild type and 35S::PID backgrounds (Figures 8E and 8F), further indicating that the polar localization of the phosphorylation mutant PIN1:GFP proteins occurred independent of PID overexpression. Consistent with the PIN1 function of mediating auxin transport to root tips, PIN1:GFP S1,3A induced an enhancement of auxin reporter DR5::GFP signal compared to the control PIN1:GFP roots (Figures 8G, 8I and 8M, Student's t-test, p < 0.05), consistent with the basal localization of PIN1:GFP S1,3A protein. In contrast, the DR5::GFP signal was significantly reduced in PIN1:GFP S1,2,3E root tips (Figure 8K and 8M, Student's t-test, p < 0.05), in line with its preferably apical localization.

In the *35S::PID* background, basally accumulated PIN1:GFP S1,3A resulted in higher auxin accumulation compared to *PIN1:GFP* (Figures 8J, 8H and 8M, Student's t-test, p < 0.05), and as a result significantly reduced the *35S::PID*-induced root collapse frequency (Figure 9C). In contrast, *PIN1:GFP S1,2,3E* had no significant effect on *35S::PID*-induced root collapse (Figure 9C). This might be due to the already maximal effect of PID overexpression on PIN apicalization and auxin depletion, as no significant reduction of auxin accumulation was detected (Figures 8B, 8F and 8M). The genetic interactions between phospho-mutants and PID confirmed that our identified serines are phosphotargets of PID.

Together, these results linked phosphorylation of the conserved serines to polar



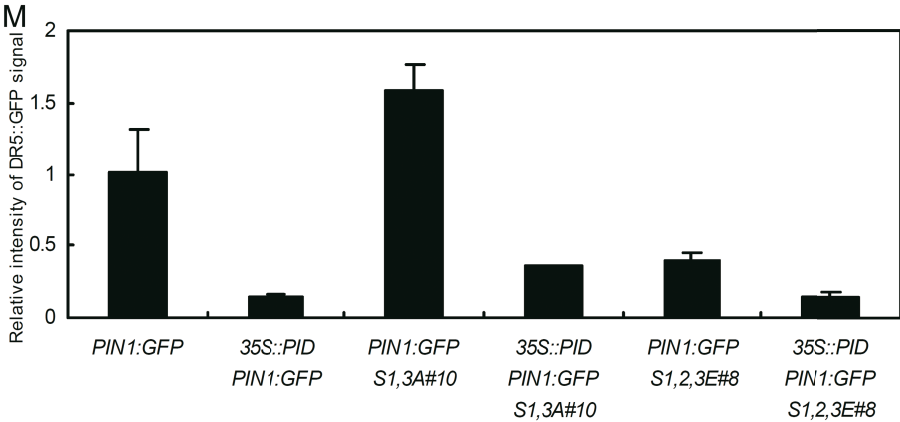


Figure 8. PIN1:GFP polarity changes induced by manipulation of phosphoserines correlate with changes in the auxin maximum in the root tip.

(A) to (F) Confocal laser scanning microscopy of primary roots of 5-day-old seedlings expressing PIN1:GFP ([A] and [B]), PIN1:GFP S1,3A#10 ([C] and [D]) and PIN1:GFP S1,2,3E#8 ([E] and [F]) in wild type ([A], [C] and [E]) or 35S::PID ([B], [D] and [F]) background. The white dashed boxes in the overview images (upper) indicate the position of the zoom-in images (lower), in which the PIN1:GFP polarity is indicated by arrows. The seedlings are homozygous for the indicated T-DNA constructs. Bars, 10 um.

(G) to **(L)** Confocal laser scanning microscopy of *DR5::GFP* signals in 3-days-old seedling root tips expressing PIN1:GFP (**[G]** and **[H]**), PIN1:GFP S1,3A#10 (**[I]** and **[J]**), and PIN1:GFP S1,2,3E#8 (**[K]** and **[L]**), in wild type (**[G]**, **[I]** and **[K]**) or 35S::PID (**[H]**, **[J]** and **[L]**) background. The seedlings are heterozygous for the *DR5::GFP* reporter. Bar, 30 um.

(M) Quantification of auxin reporter DR5::GFP expression in root tips.

PIN1 driven differential auxin distribution in roots, and further demonstrated that the conserved phosphoserines are key determinants in modulating plant architecture by instructing PIN1 polarity.

Discussion

Previously, it has been shown that the PID kinase and PP2A phosphatases antagonistically regulate PIN polarity by reversible phosphorylation of the PINHL (Michniewicz et al., 2007). However, no functional evidence was provided to support the importance of this phosphorylation *in planta*. In this study, we identified serines centrally located in three conserved TPRXS(N/S) motifs within the PIN1HL and that are phosphorylated by PID *in vitro*. Subsequent *in planta* analyses of loss-of-phosphorylation and phosphomimic *PIN1:GFP* mutants proved that reversible phosphorylation of all three residues is required and sufficient for proper PIN1 polar localization and auxin-regulated plant development.

Serines in the conserved TPRXS(N/S) motifs are crucial phosphorylation-targets in the PIN1HL

Several serine and threonine residues within the PIN1HL have been identified as phosphorylation substrates *in vivo*, and not surprisingly S2 and S3 are among them (Nühse et al., 2004; Benschop et al., 2007). Two other phosphorylation targets in the PIN1HL identified by mass spectrometry analysis are S337 and T340 in the MFSPNTG sequence (Benschop et al., 2007; Michniewicz et al., 2007). Recent functional analysis of these residues *in planta* has shown that their phosphorylation states are important for PIN1 polarity (Zhang et al., 2010). However, these residues are not directly phosphorylated by PID (Zhang et al., 2010), suggesting that other protein kinases could coordinately regulate PIN polarity with PID by phosphorylating S-337 and T-340. S-337 could be a target of mitogen activated protein kinases (MAPKs) (Benschop et al., 2007), as MAPKs preferably phosphorylate serine or threonine residues followed by a Pro in both plant and animal systems (Pearson et al., 2001; Liu and Zhang, 2004).

The TPRXS(N/S) motifs in the HL are highly conserved among six *Arabidopsis* PIN proteins (Figure 1), and among PIN1 homologs from other land plant species (Figure 3), suggesting functional conservation of the motifs. Interestingly, PID orthologs have been identified in maize and rice (McSteen et al., 2007; Morita and Kyozuka, 2007), and it has been shown that the maize ortholog BARREN INFLORESCENCE 2 (BIF2), phosphorylates ZmPIN1a, the maize ortholog of *Arabidopsis* PIN1 *in vitro*, and that it regulates the subcellular localization of ZmPIN1a *in vivo* (Skirpan et al., 2009). Further research is needed, however, to establish whether this functional conservation extends

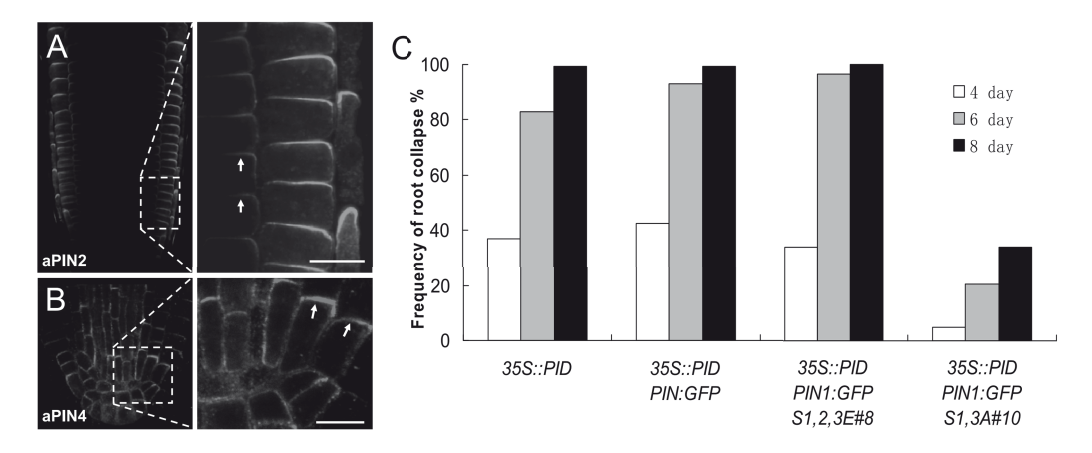


Figure 9. The effects of loss- and gain-of-phosphorylation *PIN1:GFP* mutants on *PID* overexpression-induced root collapse phenotype.

(A) and (B) PIN2 and PIN4 immunolocalization in 3-day-old P35S:PID PIN1:GFP S1,3A#10 seedling roots. The arrows indicate the apical PIN2 and PIN4 localization induced by PID overexpression. Bars, $5 \mu m$.

(C) Quantification of the effects of wild type, loss-of-phosphorylation or phosphomimic PIN1:GFP expression on the *PID* overexpression-induced root meristem collapse phenotype. Percentages are based on scoring respectively 153, 144, 179 and 98 seedlings at 4, 6 and 8 days after germination.

to the conserved TPRXS(N/S) motifs in all PIN1-type proteins in *Arabidopsis* and in other plant species.

For the *Arabidopsis* PIN1-type proteins (PIN1, 2, 3, 4 and 7), the predicted protein structure consists of two sets of five transmembrane domains that are linked by a HL (Gälweiler et al., 1998; Müller et al., 1998). On the other hand, for the PIN5-type proteins (PIN5, 6 and 8) two sets of five and four transmembrane domains, respectively, are predicted (Mravec et al., 2009). PIN5 and PIN8 clearly lack a large central HL (Mravec et al., 2009), but our alignment suggests that a shorter HL is present in PIN6 and that it contains two TPRXS(N/S) motifs (Figure 1). Immunohistochemical analyses and studies using reporter fusion proteins have shown that PIN1, 2, 3, 4 and 7 are localized at the PM (Gälweiler et al., 1998; Müller et al., 1998; Friml et al., 2002a; Friml et al., 2002b; Friml et al., 2003b), whereas, PIN5, 6 and 8 are ER-localized (Mravec et al., 2009). This suggests that for ER-localized PIN proteins there has been no selective advantage to maintain PINHL-located polarity determinants. Alternatively, the loss of phosphorylation motifs may have been crucial for allowing the diversification of PIN proteins function from the PM to the ER.

Phosphorylation of the conserved serines directs PIN1 polar localization and auxin-regulated plant development

In wild type plants, PIN1 proteins are basally localized in (pro)vascular tissues in

embryos, leaves and roots, and are apically localized in the epidermis of shoot apices and embryos (Gälweiler et al., 1998; Benková et al., 2003; Reinhardt et al., 2003; Friml et al., 2003b; Friml et al., 2004). Our analyses of the subcellular localization of mutant PIN1:GFP proteins in different tissues showed that manipulation of the phosphoserines leads to changes in PIN1 polarity, most (but not all) of which are consistent with the PID binary switch function (Friml et al., 2004).

In the epidermis of the shoot apex, loss-of-phosphorylation PIN1:GFP S1,3A and PIN1:GFP S1,2,3A proteins were targeted to the basal side (Figures 6C and 6D), whereas the phosphomimic PIN1:GFP S1,2,3E protein was apicalized (Figure 6B). This pattern is consistent with the binary switch mode, which proposes that no or low kinase activity (in the *pid* mutant) results in PIN1 localization at the basal membrane, and that above threshold kinase activity (in wild type) directs PIN1 apical localization (Friml et al., 2004). Despite its apical localization, PIN1:GFP S1,2,3E could not complement *pin1* inflorescence defects (Figure 5E), a result that is seemingly contradictory to the observation that in the shoot apex of wild type plants, PIN1 is apically localized. However, PIN1 polarity and the resulting auxin maxima in the shoot apex have been reported to be highly dynamic (Heisler et al., 2005), and a constitutively apical-localized PIN1:GFP S1,2,3E would obviously interfere with auxin-mediated organ initiation. In addition, the shoot defects could also be attributable to PIN1:GFP S1,2,3E apical localization in the vascular tissues where PIN1 polarity is normally basal.

In seedling roots, loss-of-phosphorylation PIN1:GFP S1,3A was localized on the basal membrane of root stele cells, in both wild type and 35S::PID background (Figures 8C and 8D), indicating that the protein is unresponsive to PID activity. Even though endogenous PIN2 and PIN4 in the same roots underwent the basal-to-apical polarity shift induced by PID overexpression (Figures 9A and 9B), the root collapse was delayed (Figure 9C). Previously, we have shown that pin2 and pin4 loss-of-function mutants delay P35S:PID-mediated root meristem collapse (Friml et al., 2004). It is therefore not surprising that the basally localized phosphorylation deficient PIN1 is able to reduce the frequency of root meristem collapse.

In contrast, PIN1:GFP S1,2,3E was preferably targeted to the apical membrane of root stele cells (Figure 8E). It has been shown that apical localized PIN proteins are more resistant to BFA-induced internalization (Kleine-Vehn et al., 2008a). Consistently, PIN1:GFP S1,2,3E was more resistant to BFA treatment than wild type PIN1:GFP (Kleine-Vehn et al., 2009). This, together with the reduction of the *PDR5:GFP* signal in root tips compared to that in *PIN1:GFP* roots (Figures 8K, 8G and 8M, Student's t-test, p < 0.05), strongly support that PIN1:GFP S1,2,3E predominantly localizes to the apical membrane. The apical localization of phosphomimic PIN1:GFP did not induce root meristem collapse on its own. This can be explained by the fact that the PID

overexpression-induced root meristem collapse is caused by the basal-to-apical polarity change of three PIN proteins (PIN1, PIN2 and PIN4), of which PIN2 and PIN4 are crucial players (Friml et al., 2004).

Moreover, PIN1:GFP S1,2,3E apicalization was not complete, as in certain cell files, apolar PIN1:GFP S1,2,3E localization was also detected (Figures 8E and 8F). Possibly, glutamic acid is not a perfect phosphomimic in these cell files. Alternatively, there could still be additional PID phosphorylation targets in the PIN1HL, as the S1,2,3A mutations did not completely abolish PID phosphorylation of the PIN1HL *in vitro*. Nonetheless, the basal localization of loss-of-phosphorylation PIN1 and the apical localization of phosphomimic PIN1, together with their opposite effects on PID overexpression-induced root collapse, indicated that our identified phosphoserines are functional targets of PID.

During embryogenesis, phosphorylation of the conserved serines seems to play a role in the maintenance of PIN1 PM localization rather than polarity alteration, as a complete loss of phosphorylation induces PIN1:GFP intracellular accumulation (Figures 7D and 7E). This mislocalized PIN1:GFP S1.2.3A interfered with auxin accumulation (Figures 7G and 7H), resulting in strong embryo defects (Figure 7B), similar to embryo defects of gnom and pp2aa1,3 loss-of-function (Mayer et al., 1993; Michniewicz et al., 2007), or PID gain-of-function (RPS5A>>PID) (Friml et al., 2004) mutants. The common reason for the embryo defects in these different mutants is that the basal localization of PIN1 in the provascular cells is lost, disturbing auxin accumulation in the basal tier of the embryo (Steinmann et al., 1999; Friml et al., 2004; Michniewicz et al., 2007; Figures 7G and 7H), which leads to auxin-regulated embryo defects. The enhanced intracellular accumulation of loss-of-phosphorylation PIN1 (PIN1:GFP S1,2,3A) is in line with the observation of PIN2 accumulation in endomembrane structures in pid-9 loss-of-function mutant roots (Sukumar et al., 2009), which suggests that low levels of PID activity result in intracellular accumulation of PIN proteins. Loss-of-phosphorylation-induced intracellular PIN1 accumulation might be a result of reduced recycling to the PM, or increased endocytosis, or reduced sorting from endosomes to the vacuoles. Further research is needed to distinguish between these possibilities.

AGC kinases and PIN proteins: a stable marriage in plant evolution

PID belongs to the plant specific AGCVIII family of protein kinases, which are plant orthologs of the mammalian cAMP-dependent protein kinase A (PKA), cGMP-dependent protein kinase G (PKG) and protein kinase C (PKC) (Bögre et al., 2003). Among the three identified Ser residues, two (S2 and S3) are recognized by NetPhos as PKA phosphorylation targets (Blom et al., 1999), corroborating previous suggestions that the plant AGCVIII kinases might have been derived from the same ancestral kinase as animal PKAs (Bögre et al., 2003; Galván Ampudia and Offringa, 2007).

In Arabidopsis, PID groups together with 22 other AGCVIII protein kinases (Bögre et al., 2003; Galván Ampudia and Offringa, 2007), of which the blue light receptors PHOT1 and PHOT2, the root growth regulators WAG1 and WAG2, and the D6 protein kinases (D6PKs) have also been shown to be involved in auxin transport-regulated plant development (Sakai et al., 2001; Santner and Watson, 2006; Zourelidou et al., 2009). Previously, it was shown that the PIN1HL is also phosphorylated by D6PKs (Zourelidou et al., 2009). Although the D6PKs genes showed a genetic interaction with PIN1, the D6PK protein had no effect on PIN1 polarity regulation (Friml et al., 2004; Michniewicz et al., 2007; Zourelidou et al., 2009). Further investigation into the possible D6PK phosphorylation targets in PINs should provide insight into the differential action of the distinct regulatory pathways by PID and D6PKs, PID, together with WAG1, WAG2 and AGC3-4, groups to the AGC3 clade within the AGCVIII family (Galván Ampudia and Offringa, 2007). The localization of all four kinases at the PM (Galván Ampudia and Offringa, 2007), and their genetic interactions (Cheng et al., 2008), suggest functional redundancy among the AGC3 kinases. In our studies, complete loss of phosphorylation leads to not only PID-related morphological and cellular defects, but also defects never observed in PID-regulated processes. This leads us to hypothesize that the three phosphoserines identified here are not only targets of PID, but also of other AGC3 kinases, and might explain why pid loss-of-function does not lead to apical-to-basal PIN2 polarity changes in the root (Sukumar et al., 2009), or why the strong embryo defects induced by PIN1:GFP S1,2,3A are not observed in pid mutants. Further research is needed to validate this hypothesis.

Our data, together with the conclusion that PIN proteins and PID-like kinases coevolved during the transition of plants from water to land (Galván Ampudia and Offringa, 2007), as well as the demonstrated functional relationship between PID and PINs (Friml et al., 2004), lead us to propose that phosphorylation of the conserved serines plays an important role in PIN-dependent auxin tansport throughout the evolution of plants. However, many questions still need to be answered. Functional analysis concerning phosphorylation of the three serines in other PIN proteins and the regulation of PIN proteins by other AGC kinases will be the next challenges for the coming years.

Materials and methods

Plant materials, growth conditions and phenotypic analysis

For all experiments, *Arabidopsis thaliana* of ecotype Columbia 0 (Col-0) was used. Construction of *PIN1:GFP* (to produce PIN1:GFP fusion proteins) and *P35S:PID* (to overexpress PID), and the corresponding *Arabidopsis* lines were described previously

(Benjamins et al., 2001; Benková et al., 2003). The loss-of-function alleles *pid-14* (SALK_049736) and *pin1* (SALK_047613) were obtained from the Nottingham Arabidopsis Stock Centre.

Seedlings were grown on MA medium (Masson and Paszkowski, 1992) at 21°C and a 16 hrs light/8 hrs dark photoperiod. One-week-old seedlings were transferred to MA medium supplemented with 50 uM naphthylphthalamic acid (NPA, Pfaltz & Bauer, Inc.), an auxin transport inhibitor, to induce pin-inflorescences. The number of seedlings with root meristem collapse was counted 4, 6 and 8 days after germination. Plants were grown on a mixture of 9:1 substrate soil and sand (Holland Potgrond) at 21°C, a 16 hrs photoperiod and 70% relative humidity.

DNA constructs, sequence alignment and plant transformation

Molecular cloning, DNA sequence analysis, and DNA and protein sequence alignments were performed using the Vector NTI 10 software (Invitrogen). For the in silico prediction of putative phosphorylation sites we used the NetPhos software (Blom et al., 1999). The pET-PIN1HLsv (Gälweiler et al., 1998) and pGEX-PID (Benjamins et al., 2003) constructs have been described before. The pET-PID fusion construct was generated by cloning the PID cDNA into the pET16B (Novagen) derivative pET16H, which was kindly provided by Johan Memelink. The pGEX-PIN1HL fusion was generated by cloning the PIN1HL Smal/Sall fragment from pACT2-PIN1HL into the corresponding restriction sites of plasmid pGEX-KG (Guan and Dixon, 1991). For construct pGreen0229 PPIN1:PIN1:GFP, the PIN1 gene was amplified from Col-0 DNA using primers PIN1F 5'-CGAATTCATTATTCCATTGGCGTTGTC-3' and PIN1R 5'-CAGGTACCCACTTCTTATTTTGGTGAGA-3', and the fragment was digested with EcoRI and KpnI, and cloned into the corresponding sites of pGreen0229. Subsequently, the BstAPI fragment in this genomic clone was exchanged for the BstAPI fragment containing the PIN1:GFP translational fusion from pBIN-PPIN1:PIN1:GFP (Friml et al., 2003b).

The Quickchange XL site-directed mutagenesis kit (Stratagene) was used to generate mutant constructs. Oligonucleotides used for mutagenesis are listed in Table 2. *Arabidopsis* plants were transformed by the floral dip method as described (Clough and Bent, 1998).

Protein purification and in vitro phosphorylation assays

Protein purification and *in vitro* phosphorylation assays were performed as described before (Benjamins et al., 2003; Michniewicz et al., 2007), with the following specifications. GST/HIS-tagged full-length PID and different mutant versions of GST/HIS-tagged PIN1HL proteins were used in *in vitro* phosphorylation assays. Cultures of *E. coli* strain

Table 2. Oligonucleotides used in site-directed mutagenesis

Primer names	Sequence (5' to 3')
S231A F	CGACACCTAGACCTGCGAATCTAACCAACG
S231A R	CGTTGGTTAGATTCGCAGGTCTAGGTGTCG
S231E F	CTGCGACACCTAGACCTGAGAATCTAACCAACGCTGAGATATATTC
S231E R	GAATATATCTCAGCGTTGGTTAGATTCTCAGGTCTAGGTGTCGCAG
S252A F	CCCAACGCCACGTGGCGCTAGTTTTAATCATAC
S252A R	GTATGATTAAAACTAGCGCCACGTGGCGTTGGG
S252E F	CCCAACGCCACGTGGCGAGAGTTTTAATCATAC
S252E R	GTATGATTAAAACTCTCGCCACGTGGCGTTGGG
S290A F	CCTACTCCGAGACCTGCCAACTACGAAGAAG
S290A R	CTTCTTCGTAGTTGGCAGGTCTCGGAGTAGG
S290E F	GGTCCTACTCCGAGACCTGAGAACTACGAAGAAGACGG
S290E R	CCGTCTTCTTCGTAGTTCTCAGGTCTCGGAGTAGGACC
S377,380A F	GCTCAAGTGCTGAGCCGGTCGAAGATGTGTTCGG
S377,380A R	CCGAACACATCTTCGACCGGCTCAGCACTTGAGC
S458,459A F	CGTAATCCCAACGCTTACTCCAGTTTATTCGGC
S458,459A R	GCCGAATAAACTGGAGTAAGCGTTGGGATTACG

Rosetta (Novagen) containing the constructs were grown at 37°C to OD₆₀₀=0.6 in 50 mL LC supplemented with 100 μg/mL carbenicillin, 30 μg/mL chloramphenicol and 25 μg/ mL kanamycin. The cultures were then induced for 4 hrs with 1 mM Isopropyl β-D-1thiogalactopyranoside at 30°C, after which cells were harvested by centrifugation (20 min. at 4.000 RPM, 4°C in tabletop centrifuge) and frozen in liquid nitrogen. Precipitated cells were resuspended in 2 mL Extraction Buffer (EB: 1x PBS, 2 mM EDTA, 2 mM DTT, pH 8.0) supplemented with 0.1% Tween-20 and 0.1 mM of the protease inhibitors phenylmethanesulfonyl fluoride, leupeptin and aprotinin (Sigma) and sonicated for 2 min. on ice. From this point on, all steps were performed at 4°C. Eppendorf tubes containing the sonicated cells were centrifugated at full speed (14,000 RPM) for 20 min., and the supernatants were transferred to 15 mL tubes containing 100 µL pre-equilibrated Glutathione Sepharose resin from GE Healthcare (pre-equilibration performed with three washes of EB). Resin-containing mixtures were incubated with gentle agitation for 1 hr, subsequently centrifugated at 500 relative centrifugal force (RCF) for 3 min. and the precipitated resin was washed 3 times with 20 resin volumes of EB. Then 3 resin volumes of Glutathione Elution Buffer (Reduced Glutathione 10 mM, Tris-HCl pH 8,0 50 mM) were added to the Glutathione Sepharose resin and the mixture was agitated for 10 minutes at R.T. with gentle agitation. The resin was subsequently centrifugated for 3 min. at 500 RCF and the supernatant containing the desired protein was transferred to a new tube; this process was repeated twice more. The solutions containing the proteins were diluted 1000-fold in Tris Buffer (25 mM Tris-HCl pH 7.5; 1 mM DTT) and concentrated to a workable volume (usually 50 μ L) using Vivaspin microconcentrators with a 10 kDa cut off and a maximum capacity 600 μ L (Vivascience). Glycerol was added as preservative to a final concentration of 10% and samples were stored at -80°C.

Approximately 1 μg of each purified GST/HIS-tagged protein (PID and substrates) was added to a 20 μL kinase reaction mix, containing 1x kinase buffer (25 mM Tris-HCl pH 7.5, 1 mM DTT, 5 mM MgCl $_2$) and 1 x labeled ATP solution (100 μM MgCl $_2$ /ATP; 1 μCi 32 P-γ-ATP). Reactions were incubated at 30°C for 30 minutes and stopped by addition of 5 μL of 5x protein loading buffer (310 mM Tris-HCl pH 6.8, 10 % SDS, 50% Glycerol, 750 mM β-Mercaptoethanol, 0.125% Bromophenol Blue) and boiling for 5 min. Reactions were subsequently separated over 10% acrylamide gels, which were washed three times for 30 minutes with Kinase Gel Wash Buffer (5% Trichloroacetic Acid, 1% Na $_2$ H $_2$ P $_2$ O $_7$), Coomassie stained and dried. Autoradiography was performed for 24 to 48 h at -80°C using Fuji Super RX X-ray films and intensifier screens. The relative intensity of phosphorylation bands was analyzed using ImageJ software (http://rsbweb.nih.gov/ij/).

For the peptide assays, 1µg of purified PID was incubated with 4 nmol of 9^{mer} biotinilated peptides (Pepscan) in a phosphorylation reaction as described above. Reaction processing, spotting and washing of the SAM² Biotin Capture Membrane (Promega) were performed according to the protocol of the manufacturer. Following washing, the membranes were sealed in plastic wrap and exposed to X-ray films for 24 to 48 hrs at -80°C using intensifier screens. The phosphorylation intensities of the peptides were determined by densitometry analysis of the autoradiographs using the ImageQuant software (Molecular Dynamics).

Immunolocalization, microscopy and signal analysis

Whole-mount immunolocalization was performed as described (Friml et al., 2004), using rabbit anti-PIN2 [dilution 1:200; (Abas et al., 2006)] and rabbit anti-PIN4 [dilution 1:200; (Friml et al., 2004)] as the primary antibody, and an anti-rabbit Alexa 488 conjugate as the secondary antibody (dilution 1:200; Molecular Probes).

PIN1:GFP signal in shoots and embryos and DR5::GFP signal in roots (used in Figures 7G-7L) were visualized in water without fixation. PIN1:GFP signal in 3-day-old seedling roots (used in Figures 7A-7F) was visualized with fixation and permeation steps as described (Friml et al., 2004). Signals were detected with confocal laser scanning microscopy (Zeiss LSM 5 confocal microscope). The images were processed by ImageJ software (http://rsb.info.nih.gov/ij/) and assembled in Adobe Photoshop CS2. DR5::GFP signal intensity was measured by ImageJ, and error bars were obtained based on the

measurement of three to six seedling roots per line. The Y value is the average DR5 signal intensity of each line relative to that in wild type *PIN1:GFP* line.

Embryo development was analyzed by differential intereference contrast microscopy (Zeiss Axioplan2) on cleared ovules (1 hr treatment in the clearing solution of chloral hydrate:H₂O:glycerol=8:3:1).

Accession numbers

Sequence data from this article can be found in The Arabidopsis Information Resource (http://www.Arabidopsis.org/) or GenBank/EMBL databases under the following accession numbers: *Arabidopsis* PIN1 (gi:15219501), *Arabidopsis* PIN2 (gi:42558886), *Arabidopsis* PIN3 (gi:42558887), *Arabidopsis* PIN4 (gi:42558871), *Arabidopsis* PIN6 (gi:42558888), *Arabidopsis* PIN7 (gi:42558877), *Medicago truncatula* (barrel medic) PIN1 (gi:25986771), *Oryza sativa* (rice) PIN1 (gi:75251559), *Physcomitrella patens* (moss) PIN1 (gi:55859521), and *Zea mays* (maize) PIN1 (gi:171850415). *Arabidopsis* T-DNA insertion mutants representing the loss-of-function alleles are SALK_049736 (*pid-14*) and SALK_047613 (*pin1*). Nottingham Arabidopsis Stock Centre identification numbers for the transgenic *Arabidopsis* lines *PIN1:GFP* and *P35S::PID* are N9362 and N9867, respectively.

Acknowledgements

We thank G. Lamers for technical help with confocal laser scanning microscopy, D. Doevendans for making construct *pGreen0229 PPIN1:PIN1:GFP*, S. Peck and A. Jones for providing unpublished information on mass spectrometry-detected *in vivo* phosphoresidues in the PINHL, K. Palme for kindly providing the yeast two-hybrid plasmid pACT2-PIN1HL, and A. Vivian-Smith and K. Boutilier for their helpful comments on an earlier version of the manuscript. This work was supported by grants from the China Scholarship Council (F.H.), from the Brazilian Funding Agency for Post-Graduation Education-CAPES (M.K.Z.), and from the Research Council for Earth and Life Sciences ((C.S.G.-A., ALW 813.06.004 to R.O.) and from the Research Council for Chemical Sciences (F.H., CW 700.58.301 to R.O.) with financial aid from The Netherlands Organisation for Scientific Research (NWO).